

# Inviscid and Viscous Flow Analyses of Multi-Hull Ships Under Forced Oscillations in a Free Surface

J. Chafin & P. Ananthakrishnan\*

*Department of Ocean Engineering, Florida Atlantic University, Boca Raton, FL 33431, USA*

\*Author for correspondence. email: ananth@oe.fau.edu

**ABSTRACT:** Inviscid- and viscous-flow analyses of multiple-hull ship sections under forced oscillation are carried out using boundary-integral and finite-difference methods. Both linear and nonlinear cases are considered. The nonlinear time-domain boundary-integral method is based on the mixed Eulerian-Lagrangian (MEL) formulation of Longuet-Higgins and Cokelet (1978) and the linear frequency-domain boundary-integral method on the simple source distribution method of Yeung (1974). A finite-difference method based on boundary-fitted coordinates, developed in Ananthakrishnan (1991), is used for the viscous-flow analysis. Cross comparisons of above linear, nonlinear, inviscid and viscous flow results reveal the significance of free-surface nonlinearity and viscosity in the multi-hull ship sea-keeping problem. Results also shed light on the waves generated in between the hulls and radiating away from the hulls and their effect on the hydrodynamic force. Viscous results show that vortices forming at the bilge corners can affect wave generation and hydrodynamic force, particularly at large amplitudes of oscillation.

## 1 INTRODUCTION

A multi-hull design offers several potential advantages over a mono-hull ship of similar displacement such as greater stability, better sea-keeping, and lower wave resistance. These and other advantages make the multi-hull concept a front runner among designs for fast and stable naval and commercial ships. Efficient realization of the advantages requires careful dynamic and hydrodynamic analyses to ensure, for example, that natural frequencies of ship response do not resonate with significant wave frequencies of a sea state and that waves generated by multiple hulls annul each of the other and reduce the wave resistance. Thus motivated, we have examined hydrodynamics aspects related to sea-keeping of multiple-hull sections to identify effects of principal parameters on hydrodynamic performance. The present paper reports the formulation and analysis of radiation hydrodynamics of multi-hull ship sections, including effects of viscosity and nonlinearity, and representative results highlighting the effects.

Multi-hull ship hydrodynamics is not entirely a new field of research. Various works have been carried out on resistance, sea-keeping and maneuverability of multi-hull ships. For example, Tuck and Lazouskas (1998), Peng (2001) and Yeung *et al.* (2004) have extended the Michell's thin-ship theory to analyze linear, inviscid wave resistance of multiple hull ships. Peng (2001) had also carried out linear time-domain motion response of multiple-hull ships to surface waves. McIver *et al.* (2003, 2006) conducted theoretical investigation of trapped waves associated with multi-hulls. Maiti and Sen (2001) examined nonlinear inviscid radiation problem related to single and twin hull sections.

The objectives of the research reported in this paper were to quantify effects of nonlinearity and viscosity on the interaction between waves and multiple-hulls, especially on the hydrodynamic force and radiation coefficients and to shed light on the physics of flow, particularly on the near-field flow structures and on waves generated by oscillating multiple-hull sections. The investigation was carried out using numerical methods based on boundary-integral and finite-difference algorithms. Results were obtained for a range of geometric and flow parameters to identify key parameters that could affect sea-keeping performance of multi-hull ships. An overview on the formulation and analysis and representative results and findings are presented here.

The remainder of paper is organized as follows. In Section 2, mathematical formulations of viscous and inviscid problems governing radiation hydrodynamics of multi-hull ships are presented. Linearized equations, which are valid for small-amplitude motions, and the related equations for frequency-domain analysis are also presented in Section 2. Numerical algorithms used for the analysis are reviewed in Section 3. A representative set of inviscid and viscous results is discussed in Section 4 and conclusions drawn in Section 5.

## 2 MATHEMATICAL FORMULATION

The sketch for problem definition is given in Figure 1.1. A multi-hull of beam  $B$  and draft  $d$  is forced to undergo sinusoidal motion with amplitude  $A$  and frequency  $\omega$ . The free surface is denoted as  $F$ , the body boundary as  $B$  and far-field open boundary as  $\Sigma$ . The governing equations for viscous and inviscid flows are given below.

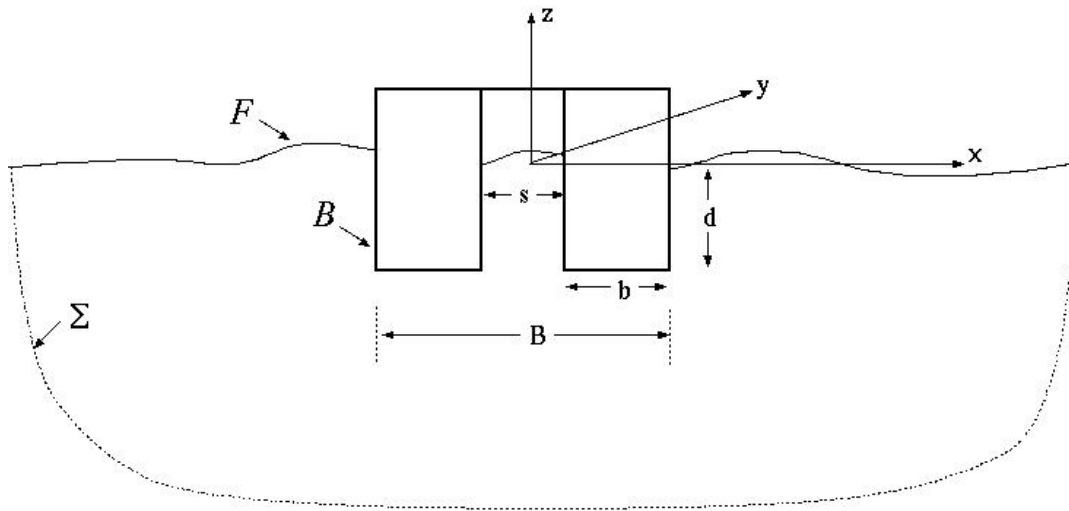


Figure 1.1 Oscillating multi-hulls in a free surface

### 2.1 Viscous Flow Formulation.

The viscous flow problem is governed by the incompressible Navier-Stokes equations:

$$\begin{aligned} \nabla \cdot \vec{u} &= 0 \\ \rho \frac{D\vec{u}}{Dt} &= \rho \vec{g} - \nabla p + \mu \nabla^2 \vec{u} \end{aligned} \quad (1)$$

where  $\vec{u}$  denotes the velocity field,  $p$  the pressure,  $\rho$  the fluid density,  $\mu$  the coefficient of dynamic viscosity and  $g$  the acceleration of gravity acting along the negative  $z$  direction.

On the body boundary underneath the surface, the no-slip/no-flux condition determines the velocity of the fluid on the body; i.e.,

$$\vec{u} = \vec{V} \text{ on the body surface, B} \quad (2)$$

A no-flux/free-slip model [Ananthkrishnan (1991)] is used to model the motion of the contact point which is the intersection of the free surface and the hull.

The time evolution of the free surface is governed by the kinematic condition of a material surface:

$$\frac{D\vec{X}}{Dt} = \vec{u} \quad (3)$$

where  $D/Dt$  represents total time derivative and  $\vec{X}$  the position vector of a free-surface particle. The free-surface dynamic condition is based on continuity of stress vector across the free surface:

$$\vec{\tau} = 0, \text{ on F} \quad (4)$$

where  $\vec{\tau} = \vec{\sigma} \cdot \hat{n}$  with  $\vec{\sigma}$  representing the stress tensor of a linear incompressible fluid. The nonlinear viscous flow problem is solved in the time domain starting from a quiescent state of zero velocity and zero free-surface elevation at initial time  $t=0$ . On the far-field open boundary  $\Sigma$ , the dynamic pressure is assumed to be zero for the duration of simulation and the velocity determined by characteristic extrapolation.

At each time step, upon solving for pressure and velocity, the hydrodynamic force on the body is determined by integrating the pressure over the body surface. The contribution of viscosity to stress is omitted, which is comparatively small, in order to make a more direct comparison with inviscid flow results and to determine the effect of viscosity on dynamic pressure.

## 2.2 Inviscid Flow Formulation

For cases in which viscosity effect is not significant, hydrodynamic analysis as inviscid flow is computationally more efficient than that as viscous flow. It is not entirely clear what parameters govern the significance of viscous effect on flow evolution, waves and hydrodynamic forces related to multi-hull ships. We therefore carry out both inviscid and viscous analyses, to determine the significance of viscosity effects by comparison of results and identify critical parameters governing viscosity effects.

We use the potential flow formulation for the inviscid flow analysis, by which fluid velocity is defined as

$$\vec{u} = \nabla \phi \quad (5)$$

where  $\phi$  denotes the velocity potential. The velocity potential, by the equation of continuity, is governed by the Laplace equation

$$\nabla^2 \phi = 0 \quad (6)$$

On the body boundary, velocity satisfies the no-flux condition:

$$\frac{\partial \phi}{\partial n} = V_n \quad (7)$$

where  $V_n$  denotes the body normal velocity.

The free-surface kinematic condition in the Lagrangian form is given by Equation (3) above. The Lagrangian form of the free-surface dynamic condition, for zero gage pressure, is given by

$$\frac{D\phi}{Dt} = \frac{1}{2} |\nabla \phi|^2 - gZ \quad (8)$$

where  $Z$  denotes the free-surface elevation.

As in the viscous-flow analysis, the nonlinear inviscid-flow analysis is also carried out in the time domain starting from rest; ie., with  $\phi = 0$  and  $Z = 0$  at time  $t = 0$ . On the open boundary  $\Sigma$  the velocity potential is assumed to be zero during the entire duration of simulation. The simulations had to be however terminated before radiated waves reach the open boundary.

### 2.3 Linear Inviscid Flow.

For small-amplitude motions, for which steady-state solutions may exist, the computations may be carried out in the frequency-domain [Yeung (1974)]. By this formulation, let the displacement of the hull under forced sinusoidal oscillation be expressed as

$$\zeta_j = A_j e^{i\omega t} \quad (9)$$

where the subscript  $j$  denotes the mode of motion,  $i$  the imaginary number,  $A_j$  the amplitude and  $\omega$  the frequency of oscillation. The corresponding velocity potential can be written as

$$\phi = \Phi_j e^{i\omega t} \quad (10)$$

where  $\Phi_j$  denotes the complex amplitude of the velocity potential corresponding to  $j$ -th mode of body motion. Similarly the free-surface elevation can be expressed as

$$Z = \eta_j e^{i\omega t} \quad (11)$$

with  $\eta_j$  representing the amplitude of free-surface elevation.

The complex amplitude of velocity potential  $\Phi_j$  satisfies the Laplace equation

$$\nabla^2 \Phi_j = 0 \quad (12)$$

and the no-flux condition on the body surface yields

$$\frac{\partial \Phi_j}{\partial n} = i\omega A_j n_j \quad (\text{on the equilibrium body surface}) \quad (13)$$

The linearized free-surface conditions in the frequency domain are given by the kinematic condition

$$i\omega \eta_j = \frac{\partial \Phi_j}{\partial z} \quad (\text{on mean surface } z=0) \quad (14)$$

and the dynamic condition

$$i\omega \Phi_j + g \eta_j = 0 \quad (\text{on mean surface } z=0) \quad (15)$$

The above conditions when combined yields

$$\frac{\partial \Phi_j}{\partial n} = \frac{1}{g} \omega^2 \Phi_j \quad (\text{on calm surface } z=0) \quad (16)$$

with  $n$  representing the outward normal ( $z$ ) direction of the calm free surface.

On the open boundary  $\Sigma$ , the velocity potential satisfies the Sommerfeld radiation condition:

$$ik\Phi_j + \frac{\partial\Phi_j}{\partial n} = 0 \quad (17)$$

where  $k$  denotes the wave number governed by the dispersion relation  $\omega^2 = gk$ .

Upon solving the above equations, methodology of which is to be reviewed in the following sections, one can determine the complex hydrodynamic force by carrying out the following integral over the mean (equilibrium) body surface:

$$f_{pq} = \rho \int_B \Phi_p n_q dS_B \quad (18)$$

One can show that

$$f_{pq} = -\omega^2 \mu_{pq} - i\omega \lambda_{pq} \quad (19)$$

where  $\mu_{pq}$  denotes the added-mass tensor and  $\lambda_{pq}$  the wave-damping tensor.

### 3 SOLUTION ALGORITHMS

The equations governing viscous and inviscid flows, presented in the earlier section, are solved numerically using finite-difference and boundary-integral methods. The viscous flow problem is solved using a boundary-fitted coordinates based finite-difference method [Ananthakrishnan (1991)]. The nonlinear potential flow problem is solved using a boundary-integral method based on mixed Eulerian-Lagrangian formulation [Longuet-Higgins and Cokelet (1976); Chafin (2007)]. The linear frequency domain analysis is carried out using a boundary-integral method based on simple source distribution [Yeung (1974)]. Overviews of these methods and algorithms are given below.

#### 3.1 Finite-Difference Method for Viscous Solution.

The incompressible Navier-Stokes equations are solved in primitive variables using a fractional-step projection method [Chorin (1968)]. In this method, at each time step, an auxiliary velocity field is determined by integrating the momentum equation either without the pressure-gradient term or with the pressure-gradient term evaluated approximately. The auxiliary field is then decomposed into the real divergence-free velocity and pressure fields.

Specifically, at each spatial node, an auxiliary velocity field is first computed by integrating the momentum equation as follows:

$$\vec{u}^* = \vec{u}^n + \delta t [D(\vec{u}^n) - C(\vec{u}^n) - \nabla P^n] \quad (20)$$

where  $\vec{u}^*$  denotes the auxiliary velocity field,  $\delta t$  the time-step size,  $C(\vec{u}^n)$  discretization of the advection terms,  $D(\vec{u}^n)$  that of the diffusion term, and  $P \equiv \frac{1}{\rho}(p + \rho g z)$ . Note that the superscript  $n$  denotes the discrete time. As pressure acts as a constraint for the velocity to be divergence-free in an incompressible flow and as the pressure term in equation (20) is only approximately evaluated based on the value at previous instant of time,  $\nabla \cdot \vec{u}^* \neq 0$ .

Next, let us consider a discretization of the momentum equation that would satisfy the equation of continuity also, as in

$$\vec{u}^{n+1} = \vec{u}^n + \delta t [D(\vec{u}^n) - C(\vec{u}^n) - \nabla P^{n+1}] \quad (21)$$

By comparing Equation (20) and Equation (21) above, we observe that

$$\vec{u}^* = \vec{u}^{n+1} + \nabla\Psi \quad (22)$$

where

$$\Psi \equiv \delta t(P^{n+1} - P^n) \quad (23)$$

denotes the pressure correction to the auxiliary velocity field. Divergence of the above gives the following Poisson equation for the pressure correction:

$$\nabla^2\Psi = \nabla\cdot\vec{u}^* \quad (24)$$

After solving the above Poisson equation for  $\Psi$  one determines the required pressure and velocity fields at discrete time (n+1) as  $P^{n+1} = P^n + \frac{1}{\delta t}\Psi$  and  $\vec{u}^{n+1} = \vec{u}^* - \nabla\Psi$ .

### 3.1.1 Boundary-Fitted Coordinates.

In order to track the moving boundaries and implement nonlinear boundary conditions accurately and to resolve flow zones of large gradients effectively, we have implemented the finite-difference method using boundary-fitted coordinates. Details on coordinate mapping and finite difference methods based on boundary-fitted coordinates can be found discussed in, for example, Ananthakrishnan (1991). In the present work, we use a reference-space based variational method, developed by Steinberg and Roache (1986) and Ananthakrishnan and Yeung (1994), for generating the boundary-fitted coordinates.

### 3.1.2 Implementation of Boundary Conditions.

In the fractional-step algorithm, the boundary conditions are implemented as follows. On the solid boundaries, both the divergence-free and auxiliary velocity fields are set to satisfy the no-slip and no-flux condition. On the free surface, a pressure Dirichlet condition is obtained using the normal-stress continuity condition. The tangential component of velocity is determined using the tangential-stress continuity condition. The equation of continuity is used to determine the normal component of velocity on the free surface. On the open boundary, dynamic pressure is assumed to be zero until waves reach the open boundary before which time the simulation was stopped. Fluid velocity was determined based on extrapolation. The decomposition relation is completed to determine the auxiliary velocity on the open boundary. For example, the results of Fekken (2004) corresponding to hydrodynamic force on a heaving mono-hull compares closely well with earlier results of Yeung and Ananthakrishnan (1992) obtained using an earlier version of the present method.

## 3.2 Boundary-Integral Method for Linear Frequency-Domain Inviscid-Flow Analysis

The Laplace equation governing the ideal flow velocity potential can be solved using the Green's theorem [Wehausen and Laitone (1960)]:

$$2\pi\phi(P) + \int_{\partial\Omega} \Phi \frac{\partial}{\partial n_Q} \frac{1}{r_{PQ}} d\partial\Omega = \int_{\partial\Omega} \frac{1}{r_{PQ}} \frac{\partial\Phi}{\partial n_Q} d\partial\Omega \quad (25)$$

where P denotes the field point and Q the singularity point. In the above,  $\Phi$  denotes the complex amplitude of the velocity potential associated with any mode of rigid-body motion. The boundary  $\partial\Omega$  includes calm free surface  $z=0$ , equilibrium body surface  $S_{Bo}$ , far-field open boundary  $\Sigma$ . Incorporating the boundary conditions, as discussed in Section 2.3 and originally given in Yeung (1974), the above integral equation can be written as

$$\begin{aligned}
2\pi\phi(P) + \int_{S_{Bo}} \Phi \frac{\partial}{\partial n_Q} \frac{1}{r_{PQ}} dS_{Bo} + \int_{z=0_o} \Phi \left( \frac{\partial}{\partial n_Q} \frac{1}{r_{PQ}} - \frac{\omega^2}{g} \right) dF_o + \int_{\Sigma} \Phi \left( \frac{\partial}{\partial n_Q} \frac{1}{r_{PQ}} + ik \right) d\Sigma \\
= \int_{S_{Bo}} \frac{1}{r_{PQ}} \frac{\partial \Phi}{\partial n_Q} dS_{Bo} \quad (26)
\end{aligned}$$

The above integral equation is solved numerically using the panel method [Chafin(2007)].

### 3.3 Boundary-Integral Method for Non-Linear Time-Domain Inviscid-Flow Analysis.

The nonlinear potential flow problem is solved using the mixed Eulerian-Lagrangian formulation of Longuet-Higgins and Cokelet (1976). In this method, at each time step, the Lagrangian form of free-surface boundary conditions, given by equations (3) and (8), are integrated to advance the free-surface position in time and to determine the velocity potential on the free surface at the new instant of time. The Green's theorem is then solved for potential on the body surface and fluid normal velocity on the free surface and open boundary. Since the body panels are not treated as Lagrangian elements, the dynamic pressure on the body surface is computed using the following generalized Euler's integral:

$$p_{dynamic} = -\rho \left[ \frac{\partial \phi}{\partial \tau} - \frac{\partial x}{\partial \tau} \frac{\partial \phi}{\partial x} - \frac{\partial y}{\partial \tau} \frac{\partial \phi}{\partial y} - \frac{\partial z}{\partial \tau} \frac{\partial \phi}{\partial z} \right] - \frac{\rho}{2} |\nabla \phi|^2 \quad (27)$$

Nonlinear, inviscid hydrodynamic force is then determined by integrating the above dynamic pressure over the body surface.

## 4 RESULTS AND DISCUSSION

Because of page limitations, we could present only one set of results in the paper. Results given Figure 4.1 correspond to heave oscillation of a catamaran of non-dimensional beam  $B = 1$ , draft  $d = 0.5$ , interior separation between demi-hulls  $S = 1$  (see Figure 1.1) and non-dimensional frequency of 2.5066. The sections are rectangular in geometry. All the parameters are non-dimensional with respect to beam, fluid density and acceleration of gravity. The amplitudes of oscillation are 0.01 in linear inviscid-flow result and 0.1 in nonlinear viscous-flow results. The Reynolds number is 01E+04 in the viscous flow simulation.

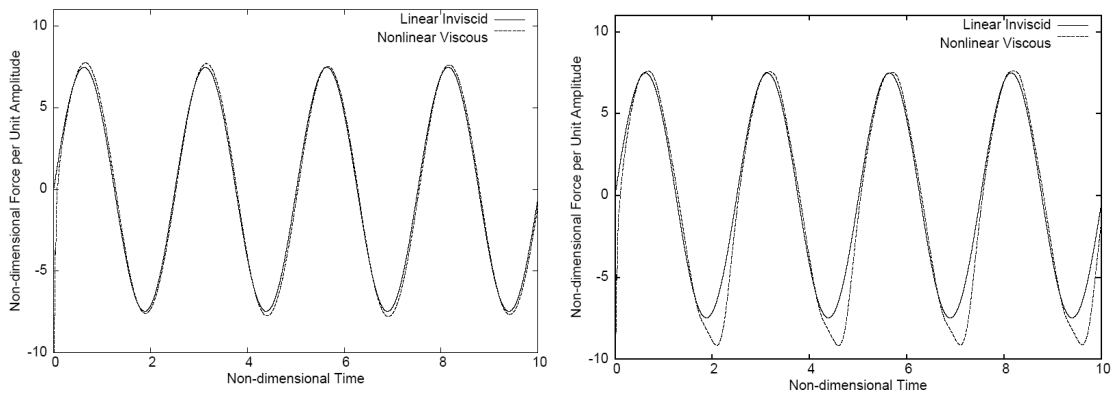


Figure 4.1 Heave force per unit amplitude of oscillation: comparison between linear inviscid and nonlinear viscous results corresponding to amplitude of oscillation 0.01 (left) and 0.1 (right) for  $B=3$ ,  $b=1$ ,  $d=0.5$ ,  $s=1$  (for definition of parameters, refer to Figure 1.1) and non-dimensional frequency =2.5066.

As can be observed from Figure 4.1 (left) that at small amplitude of oscillation the effect of non-linearity and viscosity is negligible. At large amplitude of oscillation (Figure 4.1 – right), one observes a significant difference in the hydrodynamic force. The noticeable difference is attributable to the vortices generated at the bilge corners of the catamaran.

## 5 CONCLUSION

In this paper, we presented methodologies to determine radiation hydrodynamic forces of multi-hull ships including free-surface nonlinearity and viscosity. The inviscid-flow analysis is based on boundary-integral algorithm and the viscous-flow analysis on finite-difference algorithm. A representative result presented in the paper show that viscosity effect is negligible at low amplitude of oscillation and that the noticeable difference in the hydrodynamic force observed at large-amplitude of oscillation is due to vortices forming at the bilge corners. Further findings of the research, in particular, related to trapped and standing wave modes generated between the hulls and their effects on the hydrodynamic forces will be presented at the ICHD'08 conference and published in a subsequent technical paper.

**ACKNOWLEDGEMENT:** Support for the research provided by the Office of Naval Research (ONR) through the grant N00014-03-1-0211 under the National Naval Responsibility for Naval Engineering (NNRNE) program (Program Manager: Ms. Kelly Cooper) is gratefully acknowledged.

## REFERENCES

- Longuet-Higgins, M.S. and Cokelet E.D. 1976. The deformation of steep surface waves on water: I. A numerical method of computation. *Proceedings of Royal Society, London A.*, vol. 150, pp. 1-26.
- Yeung, R.W. 1974. A Singularity Distribution Method for Free-Surface Flow Problems with an Oscillating Body. *Ph.D. Dissertation*, University of California, Berkeley.
- Ananthakrishnan, P. 1991 Surface Waves Generated by a Translating Two-Dimensional Body: Effects of Viscosity. *Ph.D. Dissertation*, University of California, Berkeley.
- Chafin, J. 2007. Determination of Hydrodynamic Coefficients of Multi-Hull Ships for Sea-Keeping Analysis. *MS Thesis*. Florida Atlantic University.
- Tuck, E.O., and Lazauskas, L. 1998. Optimum spacing of a family of multi-hulls. *Schiffstechnik*, Vol. 45, No. 4, pp. 180-195.
- Peng, H. 2001. Numerical Computation of Multi-Hull Ship Resistance and Motion, *Ph. D. Dissertation*, Department of Naval Architecture, Dalhousie University.
- Yeung, R. W., Poupard, G. and Toilliez, J. 2004. Interference-resistance prediction and its applications to optimal multi-hull configuration design. *SNAME Maritime Technology Conference*, Paper D41, Washington, D.C.
- McIver, P. & McIver, M. 2006 Trapped modes in the water-wave problem for a freely floating structure. *Journal of Fluid Mechanics* 558, pp.53-67.
- McIver, P., McIver, M. & Zhang, J. 2003 Excitation of trapped water waves by the forced motion of structures. *Journal of Fluid Mechanics*, 494, pp. 141-162.
- Maiti, S. and Sen, D. 2001. Nonlinear heave radiation forces on two-dimensional single and twin hulls. *Ocean Engineering* 28, pp. 1031-1052.
- Chorin, A. J. 1968. Numerical solution of the Navier-Stokes equations. *Mathematics of Computation*, 22, 745-762
- Ananthakrishnan, P. and R. W. Yeung. 1994. Nonlinear interaction of a vortex pair with clean and surfactant-covered free surfaces. *Wave Motion*, 19, 343-365.
- Steinberg, S. and Roache, P.J. 1986. Variational grid generation. *Numerical Methods in Partial Differential Equations*, 2, 71-96.
- Fekken, G. 2004. Numerical Simulation of Free Surface Flow with Moving Rigid Bodies. *Ph.D. Dissertation*, University of Groningen, The Netherlands.
- Yeung, R. W. and Ananthakrishnan P. 1992. Oscillation of a floating body in a viscous fluid. *Journal of Engineering Mathematics*, 26., 211-230.
- Wehausen, J.V. and Laitone, E.V. 1960. Surface Waves. *Handbuch der Physik*, ix, Springer, Germany.